Hydrated Positive Ions in Nitric-Oxide–Water Afterglows

W. C. Lineberger* and L. J. Puckett
Ballistic Research Laboratories, U. S. Army Aberdeen Research and Development Center, Aberdeen Proving Ground, Maryland 21105
(Received 10 June 1969)

Results of measurements performed on a stationary NO–H_2O afterglow are reported in this paper. The gas mixture was contained in a large, gold-plated, cylindrical chamber in which the NO was ionized by means of krypton resonance radiation. The ions from the afterglow were sampled through an electrically insulated orifice and were quantitatively detected by time-resolved mass spectrometry. For NO^+ ions reacting in NO–H_2O mixtures at 295 K, the product-ion mass spectrum is dominated by NO^+ and its hydrates, $NO^+ \cdot nH_2O$, and by hydrated hydronium, $H_3O^+ \cdot nH_2O$. The sequence of reactions leading to these products has been determined, and the rate constant for the three-body conversion of NO^+ to $NO^+ \cdot H_2O$ has been measured to be $(1.5 \pm 0.5) \times 10^{-28}$ cm^6/sec. Bounds for several other rate constants in the reaction sequence have been obtained. The ions $H_3O^+ \cdot 2H_2O$, $H_3O^+ \cdot 3H_2O$, and $H_3O^+ \cdot 4H_2O$ observed in the afterglow are of the same family as the hydronium ion H_3O^+ and its hydrates $H_3O^+ \cdot H_2O$ and $H_3O^+ \cdot 2H_2O$, which are prominent in the *D* region of the ionsphere. Reaction sequences similar to the one reported in this paper, which involve multiply hydrated atmospheric ions, may be an important contributors to the production of the hydrated hydronium observed in the ionosphere.

I. INTRODUCTION

Recent rocketborne mass spectrometer observations[1,2] of the positive ions in the *D* region of the ionosphere have established that water-clustered ions (e.g., $H_3O^+ \cdot nH_2O$) may play a decisive role[3] in *D*-region chemistry. In addition to the water-clustered hydronium series, which is frequently observed in the laboratory,[4] several groups have recently reported mass spectrometric detection of water clusters on NO^+,[5–7] NO_2^+,[5] NO_2^-,[8] O_2^+,[5,6] O^-,[9] and O_2^-[9] ions. In none of these cases have the rate constants for cluster formation been reported.

One reason for which these clustered ions are important is that the presence of a loosely bound neutral on an ion generally increases the ion-electron dissociative recombination coefficient. For example, Biondi and co-workers[10,11] found the dissociative recombination coefficients of both N_4^+ and $NO^+ \cdot NO$ to be about a factor of 5 larger than those of N_2^+ and NO^+, respectively. The formation of clusters on atomic ions may increase the recombination coefficient by several orders of magnitude, since dissociative recombination channels are opened to compete with radiative, collisional radiative, or dielectronic recombination.

Since the presence of these clusters may have a significant effect on the chemical kinetics of the lower ionosphere, we have initiated a program to investigate water-clustering mechanisms for positive and negative ions of atmospheric interest. In this program the measurements are made by means of a stationary afterglow apparatus. This paper reports the formation mechanisms and rate constants for production of $NO^+ \cdot H_2O$ ions in photoionized NO–H_2O mixtures. In addition, results are presented concerning the formation of the $H_3O^+ \cdot H_2O$ series in NO–H_2O mixtures under conditions where the initial ionic species is NO^+, and direct photoionization of H_2O is energetically impossible.

II. EXPERIMENTAL

The basic apparatus employed in these experiments is the photoionization stationary afterglow instrument described previously,[12] and only a brief account of the apparatus will be presented here. A schematic diagram of the apparatus is shown in Fig. 1.

The afterglow cavity is an ultrahigh-vacuum bakeable gold-coated–stainless-steel cylinder 18 in. diam and 36 in. long. Information on the individual ion species in the plasma afterglow is obtained by means of time-resolved mass spectrometry of the ions which pass through a 0.60-mm-diam sampling orifice in the cavity wall. The sampling orifice is contained in a plate which is contoured to the shape of the cavity wall and electrically isolated from the wall. In this investigation the plate potential was set ~100 mV negative with respect to the wall.[13]

The primary NO^+ ions are produced by photoionization of NO with krypton resonance radiation (123.6 and 116.5 nm) from a pulsed microwave powered discharge lamp. The lamp is coupled to the afterglow cavity through a 1-mm-thick MgF_2 window which transmits approximately 50% of the radiation at these wavelengths. The MgF_2 trans-

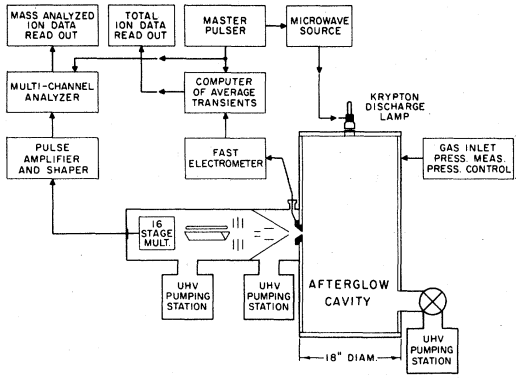

FIG. 1. Schematic diagram of stationary afterglow apparatus.

mission cutoff at ~115 nm precludes the possibility of direct photoionization of H_2O (threshold 98.4 nm) in the NO-H_2O mixtures. Initial ion densities were varied below 10^7 cm^{-3} to ensure that ionic recombination losses contributed negligibly to the ion decay.

The monopole mass filter has excellent resolution and sensitivity so that one can calibrate the control settings for ions up to $m/e > 100\ m_H/e$ by counting mass peaks in a spectrum created by operating the spectrometer as a residual gas analyzer. In addition, the chemical identification of reaction products containing H_2O was verified by substitution of D_2O and $H_2{}^{18}O$.

The NO and H_2O pressures in the cavity were measured with a capacitance manometer. The NO and H_2O were added separately to the cavity without premixing. Normal H_2O concentrations were 0.1–5.0%, with the remainder of the gas being NO. The procedure utilized is as follows: With the cavity evacuated, H_2O is admitted through a variable leak valve, and a dynamic equilibrium is established between H_2O entering the cavity and H_2O being pumped out through the ion sampling orifice. Since the cavity time constant is long compared with the capacitance-manometer time constant, the H_2O equilibrium pressure can be directly measured. After the H_2O pressure has equilibrated, NO gas is added to obtain the desired total pressure. Measurements are taken in a time short compared to the cavity pumpout time in order to avoid possible changes in gas composition. In spite of these precautions, the H_2O pressure following addition of NO is greater than the equilibrium H_2O pressure prior to addition of NO. This increase appears to be due to desorption of H_2O from the cavity walls upon addition of NO. The increase, while representing an H_2O desorption of only a fraction of a monolayer, is a significant fraction of the total H_2O pressure and must be accounted for by means of differential H_2O pressure measurements, as described in Sec. III.

III. DATA ANALYSIS

If the dominant loss processes for NO^+ ions in dilute H_2O-NO mixtures are ambipolar diffusion and the reactions

$$NO^+ + NO + NO \xrightarrow{k_1} NO^+ \cdot NO + NO\ , \tag{1}$$

and

$$NO^+ + H_2O + NO \xrightarrow{k_2} NO^+ \cdot H_2O + NO\ , \tag{2}$$

then, for a fundamental mode distribution in a cylindrical cavity of radius R cm, the NO^+ density in the afterglow may be expressed by[11]

$$[NO^+(r,t)] = [NO^+(0,0)] J_0 2.405 r/R)\ \exp\left[-\left(\frac{D_a p}{\Lambda^2 p}\, t\right)\right.$$

$$\left. - (k_1\ NO\ ^2 t) - (k_2[NO][H_2O]t)\right]\ , \tag{3}$$

where [ ] denotes number density in cm^{-3}, $[NO^+(0,0)]$ is the initial axial number density, p is the total pressure, and Λ is the characteristic diffusion length of the afterglow cavity. The quantities k_1 and k_2 are reaction rate constants (units of cm^6/sec), and D_a is the NO^+ ion-electron ambipolar diffusion coefficient. It is also assumed in the derivation of Eq. (3) that there are no sources of NO^+ ions during the afterglow.

It can be shown that, under proper experimental conditions,[12] the count rate of the sampled, mass-analyzed NO^+ ions is directly proportional to the NO^+ volume number density. If the reciprocal time constant of the exponential NO^+ decay is denoted by ν, then

$$\nu = \frac{D_a p}{\Lambda^2 p} + k_1[NO]^2 + k_2[NO][H_2O]$$

$$= \nu_{NO} + k_2[NO][H_2O]\ . \tag{4}$$

For negligibly small H_2O concentrations, ν_{NO} is the observed NO^+ loss frequency in pure NO, a quantity which has been measured previously.[12] A plot of $\nu - \nu_{NO}$ as a function of $[NO][H_2O]$ will indicate the dependence of the reaction on the NO and H_2O pressures, and from this information one can evaluate the rate constant k_2. As a result of H_2O desorption from the cavity upon addition of NO, it proved advantageous to observe changes in the NO^+ loss frequency as a function of changes in H_2O concentration at fixed NO concentration. If two H_2O concentrations $[H_2O]_1$ and $[H_2O]_2$ are both small compared with $[NO]$, then the change in NO^+ loss frequency, $\Delta\nu$, is given by

$$\Delta\nu = k_2[NO]\{[H_2O]_2 - [H_2O]_1\}$$

$$= k_2[NO]\Delta[H_2O]\ . \tag{5}$$

Since, in each case, H_2O is first added to the cavity to the desired pressure, and H_2O equilibrium with the cavity walls is established, the differential measurement provides approximate cancellation of the H_2O description which occurs upon addition of NO. Most of the data reported here were taken in this fashion, although for $[H_2O]/[NO] \geq 0.04$, the rate constants calculated from either direct or differential water pressure measurements were in agreement.

IV. EXPERIMENTAL RESULTS

In pure NO, at 295 K the dominant positive ions are NO^+ and the $NO^+ \cdot NO$ dimer. The dimer is formed from NO^+ in a three-body reaction with a rate constant[12] of $(5 \pm 1) \times 10^{-30}$ cm^6/sec. Upon addition of a small amount ($\sim 0.1\%$) of H_2O to the NO, the $NO^+ \cdot H_2O$ ion becomes a prominent ion in the afterglow. However, at these low H_2O concentrations the major source of $NO^+ \cdot H_2O$ is from the reversible reaction

$$NO^+ \cdot NO + H_2O \underset{k_4}{\overset{k_3}{\rightleftarrows}} NO^+ \cdot H_2O + NO \ . \qquad (6)$$

This conclusion is based upon the following observations: (i) $[NO^+]$ in continuous irradiation did not appreciably change upon addition of trace amounts of H_2O. (ii) $[NO^+ \cdot NO]$ decreased markedly upon addition of H_2O, and the sum of $[NO^+ \cdot NO]$ and $[NO^+ \cdot H_2O]$ following addition of H_2O was equal to $[NO^+ \cdot NO]$ prior to H_2O addition. (iii) Upon addition of H_2O the NO^+ loss frequency did not change sufficiently to account for more than a small fraction of the $NO^+ \cdot H_2O$ being formed directly from NO^+.

(iv) The $NO^+ \cdot NO$ and $NO^+ \cdot H_2O$ afterglow decays had the same decay constants, which, together with observation (ii), imply that equilibrium concentrations were established between these two ions.

Figure 2 shows typical afterglow decay curves for $NO^+ \cdot NO$ and $NO^+ \cdot H_2O$ ions at an H_2O partial pressure of 1 mTorr and NO pressure of 100 mTorr. From the observation that these two ions appear to reach an equilibrium in ~ 10 msec, and the known H_2O concentration, it follows that $k_3 > 10^{-12}$ cm^3/sec. Moreover, the reverse reaction, conversion of $NO^+ \cdot H_2O$ to $NO^+ \cdot NO$, must also be occurring, although the rate constant k_4 must be $\sim 10^{-3}\ k_3$. Also shown in Fig. 2 are typical afterglow decays for NO^+ and $NO^+ \cdot 2H_2O$, the latter becoming more important as water concentration is increased.

The loss frequency obtained from the data in Fig. 2 provides one of the two loss frequencies required for the differential water-concentration rate-constant measurement described in Sec. III. The results of a number of such measurements are shown in Fig. 3 in which $\Delta\nu$ for NO^+ is plotted as a function of $[NO]\,\Delta\,[H_2O]$. The dependence is linear and implies a rate constant of 1.5×10^{-28} cm^6/sec for the reaction

$$NO^+ + H_2O + NO \underset{}{\overset{k_2}{\rightleftarrows}} NO^+ \cdot H_2O + NO. \qquad (2)$$

It is also necessary, however, to demonstrate that $\Delta\nu$ is linear with both $[NO]$ and $\Delta[H_2O]$. Figure 4 depicts $\Delta\nu/[NO]$ as a function of $\Delta\,[H_2O]$; the dependence is indeed linear, and together with the linearity with $[NO]\Delta[H_2O]$ establishes linearity of $\Delta\nu$ individually with both $[NO]$ and $\Delta[H_2O]$. These data were all taken using the differential H_2O-

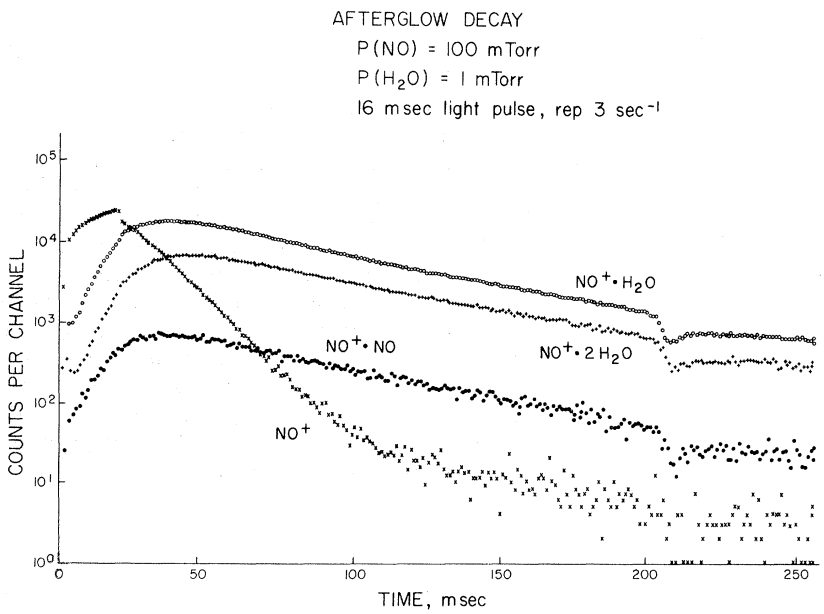

FIG. 2. Typical afterglow curves for NO^+, $NO^+ \cdot NO$, $NO^+ \cdot H_2O$, and $NO^+ \cdot 2H_2O$ ions in an NO pressure of 100 mTorr and an H_2O pressure of 1 m Torr.

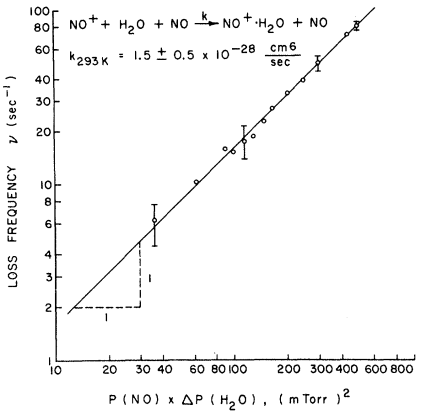

FIG. 3. Variation of NO^+ loss frequency as a function of the product of NO and H_2O pressures.

pressure measurement described, previously. However, direct measurements using the analysis implied in Eq. (4) yielded identical results for H_2O pressures greater than ~4 mTorr. For lower H_2O pressure, desorption of H_2O from the cavity walls upon addition of NO increased the H_2O concentration appreciably above the measured concentration and caused the NO^+ loss frequency to appear too large. The reaction rate constant with argon substituted for NO in reaction (2) was also crudely measured. The rate constant so determined did not differ appreciably from that measured with NO as the third body. All measurements were made at temperatures near 295 K.

The major uncertainty in the determination of k_2 is the H_2O-pressure measurement. The accuracy of the determination of $[H_2O]$ at pressures greater than 4 mTorr is estimated to be ±20%. The uncertainty increases with decreasing $[H_2O]$ until for pressures less than 0.5 mTorr wall desorption makes the measurements only qualitative. Since k_2 can be determined from the higher water-pressure data, only the 20% uncertainty enters into the result. Other uncertainties in the data from this apparatus have been discussed previously,[12] and add another ±12% to the uncertainty. Thus, the value for k_2 has been determined to be $(1.5 \pm 0.5) \times 10^{-30}$ cm⁶/sec.

The addition of water to the afterglow cavity also produced two families of positive ions at $M/e = 18$, 36, 54 and 55, 73, 91. Through isotopic substitution (e.g., D_2O for H_2O and $H_2{}^{18}O$ for $H_2{}^{16}O$) the 55, 73, 91 sequence has been verified to be part of the $H_3O^+ \cdot nH_2O$ sequence. Employing the same isotopes, the ions in the 18, 36, 54 family were shown to contain O and H in the proper abundance to be consistent with the interpretation[6] that these ions are H_2O^+, $H_3O^+ \cdot OH$, and $H_3O^+ \cdot OH \cdot H_2O$. This investigation, however, did not yield any direct information on the structure of these molecular ions. The development of these two families of ions as a function of NO and H_2O pressure is depicted in Figs. 5 and 6. The dominant production of $NO^+ \cdot H_2O$ from $NO^+ \cdot NO$ and not from NO^+ is evidenced by these data.

Figure 7 depicts the afterglow behavior of a number of these ions at an NO pressure of 50 mTorr and an H_2O pressure of 4.0 mTorr. It should be noted that an equilibrium appears to be established between masses 55, 73, and 91. Also,

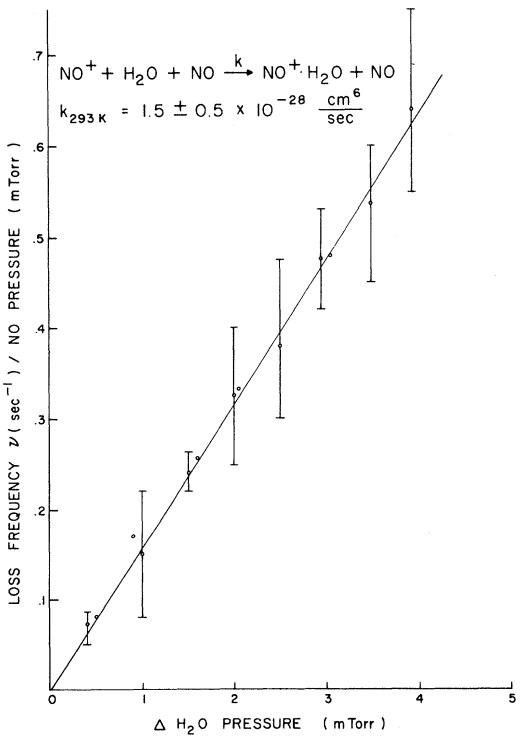

FIG. 4. Variation of the NO^+ loss frequency divided by the NO pressure versus H_2O pressure.

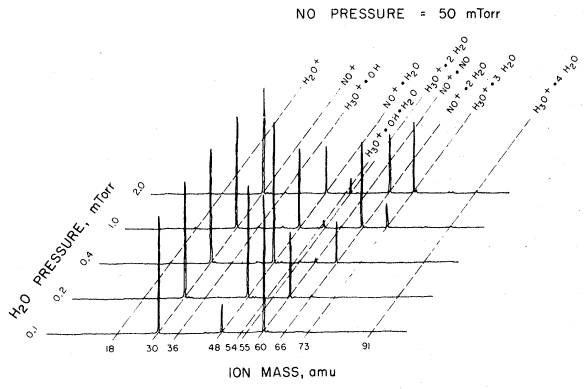

FIG. 5. Evolution of the ion spectrum as a function of increasing H_2O pressure in NO at 50 mTorr. The integrated spectrum for each gas pressure is normalized to the same value.

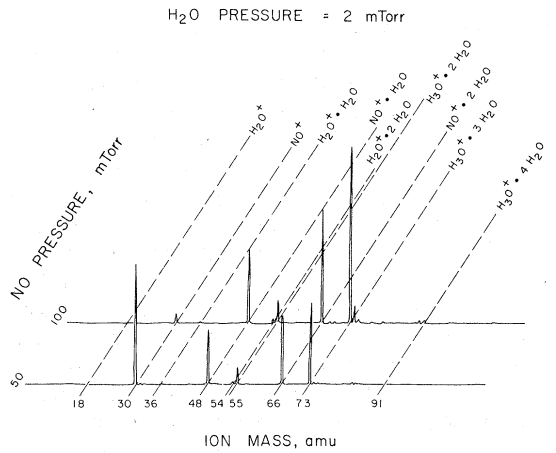

FIG. 6. Evolution of the ion spectrum as a function of increasing NO pressure in H_2O at 2 mTorr. The integrated spectrum for each gas pressure is normalized to the same value.

at early times in the afterglow, recombination loss is evident in this family of ions. Masses 36 and 54 are another family of ions which appear to be in equilibrium. Mass 18 (H_2O^+) is not thought to be produced through gas-phase chemistry as are the other ions. Instead, it is believed that 18 (H_2O^+) is produced by chemistry involving the ions and the water-coated chamber wall. This conclusion is based on the following observations. (a) The abundance of mass 18 (H_2O^+) depends strongly on the past exposure of the chamber walls to water vapor. (b) Masses 19 (H_3O^+) and 37 ($H_3O^+ \cdot H_2O$), which would be produced through gas-phase chemical reactions of H_2O^+ with water, are absent. (c) The mass 18 (H_2O^+) afterglow decay tracks the prominent ions 48 ($NO^+ \cdot H_2O$) and 66 ($NO^+ \cdot 2H_2O$) (not shown in Fig. 7 for simplicity).

Whenever equilibrium is established within a family of ions, it causes difficulties with quantitative interpretation of the decays. Such difficulties arise because the decay is not simply characteristic of the ionic loss processes, as there are obviously sources available for most ions at all times in the afterglow.

Several points concerning the data need to be made. First, the immediate source of the ions $H_3O^+ \cdot OH$, $H_3O^+ \cdot OH \cdot H_2O$, and the series $H_3O^+ \cdot nH_2O$ would appear to be $NO^+ \cdot nH_2O$. The original source, however, of all the ions observed is NO^+; this point was demonstrated by the conspicuous absence of all ionization when NO was replaced by argon in the chamber. The substitution of argon for NO also verified that the water-ion sequence was not formed through direct photoionization of water molecules. Neither does the water-ion sequence come directly from NO^+, because the observed loss frequency of NO^+ under all conditions is accounted for by reactions (1) and (2) and ambipolar diffusion. Finally, our observations indicate that the $NO^+ \cdot nH_2O$ series of ions all have an unknown but fast loss channel open at times when the $H_3O^+ \cdot nH_2O$ series is observed.

The $H_3O^+ \cdot nH_2O$ ions observed all have loss frequencies very close to the expected diffusion loss frequency. Any charge transfer between these ions and NO must be proceeding with a rate constant at least three or four orders of magnitude slower than the gas kinetic rate constant. This result indicates that the charge transfer process between $H_3O^+ \cdot nH_2O$ ($n = 2, 3$) and NO is probably endothermic.

The $H_3O^+ \cdot H_2O$ ion is not observed in our apparatus, although the ion is commonly observed in air discharges. It is possible that these ions are formed in our apparatus, but are lost by charge transfer to NO. Since in our apparatus an ion undergoes typically 10^5 or more collisions before reaching the wall, any ion with a fast two-body loss process involving NO would be unlikely to survive long enough to reach the sampling orifice.

V. DISCUSSION

The $NO^+ \cdot H_2O$ ion can be formed both in a two-body reaction between $NO^+ \cdot NO$ and H_2O and a three-body reaction involving NO^+, H_2O, and a third body. The three-body rate constant is $(1.5 \pm 0.5) \times 10^{-28}$ cm^6/sec with NO as the third body. Only the three-body reaction is likely to be of atmospheric importance. The ion observed by Narcisi at $m/e = 48$ with his D-region mass spectrometer is very likely $NO^+ \cdot H_2O$.

It has been recognized for some time that a serious energetics problem arises[14] in attempting to

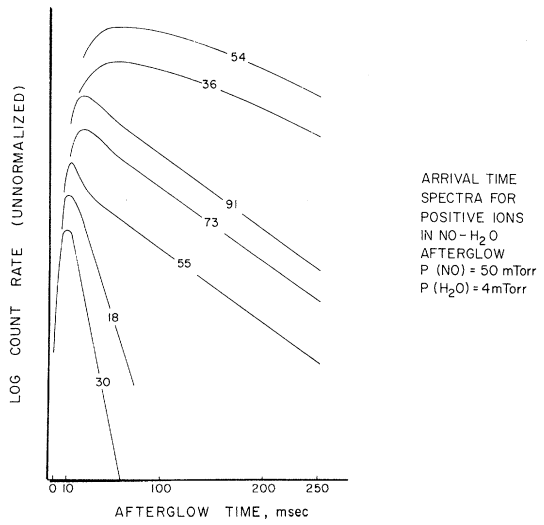

FIG. 7. Characteristic afterglow behavior of the ions formed by clustering to H_2O^+ and H_3O^+.

account for the presence of large numbers of H_3O^+ and $H_3O^+ \cdot H_2O$ ions in the lower *D* region of the ionosphere. Essentially, some mechanism involving prominent atmospheric ions is required to produce H_3O^+ and its hydrates. A reaction sequence which involves H_2O^+ fails because of the charge transfer channels open to N_2 and O_2. It has been postulated[14] that these ions are produced by photoionization of neutral water clusters by radiation longer than 121.6 nm. Our results indicate that it is also possible to produce at least portions of the $H_3O^+ \cdot nH_2O$ sequence by means of water-clustered NO^+ ions. The following sequence is proposed[15] as the mechanism by which $H_3O^+ \cdot nH_2O$ are produced in this experiment.

$$NO^+ + NO + NO \rightarrow NO^+ \cdot NO + NO \ , \quad (7)$$

$$NO^+ + H_2O + NO \searrow \quad (8)$$

$$NO^+ \cdot H_2O + NO \ , \quad (9)$$

$$NO^+ \cdot NO + H_2O \nearrow$$

$$NO^+ \cdot nH_2O + H_2O + (M) \rightarrow NO^+ \cdot (n+1)H_2O + (M) \ , \quad n = 1, 2 \quad (10)$$

$$NO^+ \cdot (n+2)H_2O + H_2O \rightarrow H_3O^+ \cdot (n+1)H_2O + HNO_2 \ , \quad n = 1, 2 \quad (11)$$

$$H_3O^+ \cdot (n+1)H_2O + H_2O + (M) \rightarrow H_3O^+ \cdot (n+2)H_2O + (M) \ , \quad n = 1, 2 \quad (12)$$

In reactions (10) and (12), (M) is used to indicate that we have no direct information regarding whether or not a third body plays an important role in these reactions.

A further separate confirming observation that the reactions are proceeding as indicated in Eqs. (7)–(12) is that the neutral product of (11), HNO_2, has been detected. HNO_2, like H_2O, readily attaches to negative ions such as NO_2^- and HCO_3^-. In this experiment the ions of $NO_2^- \cdot nHNO_2$ and $HCO_3^- \cdot nHNO_2 (n=0, 1, 2)$ are quite prominent for H_2O pressures around 5 mTorr in NO at 0.5 Torr. Similar clustering of HNO_2 to some positive ions has recently been observed, but not to the extent observed for negative ions. Tests have been performed to ensure that the HNO_2 is not being produced through the reaction

$$NO + NO_2 + H_2O \rightarrow 2HNO_2$$

as suggested by Kerbarle *et al.*[4] The negative-ion measurements will be discussed further in a subsequent publication.

Recently, Fehsenfeld and Ferguson[6] have found that O_4^+ reacts with H_2O in a manner similar to that of $NO^+ \cdot NO$ [Eqs. (7)–(12)]. Perhaps the most significant difference between the NO^+ and O_2^+ reactions with H_2O is that only two clustered water molecules on O_2^+ are required to open a channel for producing hydronium, whereas four water molecules are required in the case of NO^+. The O_2^+ reaction sequence should be of greater importance in *D*-region chemistry, primarily because of the shorter reaction chain involving $O_2^+ \cdot nH_2O$. The reaction sequence (7)–(12) illustrates the manner in which the hydrated hydronium ions are produced in this laboratory apparatus. While the mechanism is also operative in the *D* region, it appears that, as far as *D*-region kinetics are concerned, the most important clustered ion in this sequence is $NO^+ \cdot H_2O$ and that the $H_3O^+ \cdot nH_2O$ ions are produced primarily through O_2^+.

---

*Present Address: Joint Institute for Laboratory Astrophysics, University of Colorado, Boulder, Colo.

[1]R. S. Narcisi, and A. D. Bailey, J. Geophys. Res. 70, 3687 (1965).

[2]R. A. Goldberg, and L. J. Blumle, Trans. Am. Geophys. Union 50, 269 (1969).

[3]E. E. Ferguson, Rev. Geophys. 5, 305 (1967); E. E. Ferguson (private communication).

[4]M. N. Hirsh, P. N. Eisner, G. M. Halpern, and J. A. Slevin, Report No. R-199-1, The G. C. Dewey Corporation, 1965 (unpublished); M. M. Shahin, J. Chem. Phys. 47, 4392 (1967); E. E. Ferguson (private communication); P. Kerbarle, S. K. Searles, A. Zolla, J. Scarborough, and M. Arshadi, J. Am. Chem. Soc. 89, 6393 (1967).

[5]M. M. Shahin, J. Chem. Phys. 45, 2600 (1966).

[6]F. C. Fehsenfeld, and E. E. Ferguson, J. Geophys. Res. 74, 2217 (1969); A. N. Hayhurst and P. J. Padley, Trans. Faraday Soc. 63, 1620 (1967).

[7]T. A. Milne (private communication).

[8]W. L. Fite and J. A. Rutherford, Report No. GA-4867, General Atomic, 1963 (unpublished).

[9]J. L. Moruzzi and A. V. Phelps, J. Chem. Phys. 45, 4617 (1966).

[10]M. A. Biondi, T. R. Connor, S. C. Weller, and W. H. Kasner, Technical Report No. 3, Office of Naval Research, 1964 (unpublished).

[11]C. S. Weller and M. A. Biondi, Phys. Rev. 172, 198 (1968).

[12]W. C. Lineberger and L. J. Puckett, Phys. Rev. (to be published).

[13]We have determined that the orifice potentials has a marked effect on the *observed* ion decay. The potentials utilized in this work are such as to produce an uncertainty of less than 10% in the relationship of the observed and the actual decays. See Ref. 12 for a more complete descritpion of this effect.

[14]R. S. Narcisi, Ann. Geophys. 22, 224 (1966).

[15]Essentially the same scheme was proposed by E. E. Ferguson at the Third Aeronomy Conference, Urbana, Illinois, 1968 (unpublished).